Cellular and Molecular Life Sciences (2022) 79:233
https://doi.org/10.1007/s00018-022-04245-x

ORIGINAL ARTICLE

Mapping of molecular interactions between human E3 ligase TRIM69 and Dengue virus NS3 protease using hydrogen–deuterium exchange mass spectrometry

Tanaya Bagga[1] · Nikhil Kumar Tulsian[1,2] · Yu Keung Mok[1] · R. Manjunatha Kini[1,3,4] · J. Sivaraman[1]

Received: 22 December 2021 / Revised: 4 March 2022 / Accepted: 10 March 2022 / Published online: 10 April 2022

Abstract

Tripartite motif (TRIM) E3 ligases target specific substrates, including viral proteins, for proteasomal degradation, and are thus essential regulators of the innate antiviral response. TRIM69 ubiquitinates the non-structural NS3 protein of Dengue virus for its degradation by the host machinery. This antiviral strategy abrogates the immunosuppression mediated by the NS2B–NS3 protease complex. To understand how this host-driven antiviral response against Dengue virus, we sought to define the mode of interaction between human TRIM69 and Dengue NS2B–NS3 and the subsequent polyubiquitination of the protease by the E3 ligase. We show that NS2B–NS3Δpro is sufficient as a substrate for ubiquitination by TRIM69 using ELISA and in vitro assays. Using hydrogen–deuterium exchange mass spectrometry (HDXMS), we mapped the interface of the interaction between TRIM69 and NS2B–NS3Δpro, and propose a rationale for the binding and subsequent ubiquitination process. Furthermore, through sequence analysis, we showed that the regions targeted by TRIM69 on the DENV-2 NS3 protease (NS3Δpro) are well conserved across DENV serotypes and other flaviviruses, including Zika virus, West Nile virus, and Japanese encephalitis virus. Our results show the direct interactions of TRIM69 with viral proteins, provide mechanistic insights at a molecular level, and highlight the functional relevance of TRIM69 interacting with the Dengue viral protein. Collectively, our findings suggest that TRIM69 may act as a pan-antiflaviviral restriction factor.

Keywords TRIM69 · NS2–NS3 protease · HDXMS · Antiviral mechanism · Dengue virus

Introduction

Mosquito-borne viral infections, such as Dengue are endemic to subtropical and tropical climates [1]. Upon entry into the cell, Dengue virus (DENV) hijacks the host cell machinery to translate the genomic RNA into a polyprotein, the cleavage of which by host and viral proteases leads to the formation of various structural and non-structural (NS) proteins [2]. Of the various NS proteins, NS3 is of particular importance, as it is responsible for proteolysis of the polyprotein via its N-terminal serine protease domain (NS3pro) [3]. However, it requires complexation with a hydrophilic segment of 18 residues from NS2B as cofactor to form a proteolytically active NS2B–NS3 protease complex [4–6]. Indeed, studies suggest that flaviviral replication can be disrupted by inhibiting NS2B–NS3pro function [7].

Concurrently, following entry into the cell, Dengue virus (DENV) is recognized by cognate innate immune receptors, which trigger the activation of the Type I Interferon system and the production of antiviral interferon-stimulated

✉ Nikhil Kumar Tulsian
nikhil.tulsian@nus.edu.sg

✉ J. Sivaraman
dbsjayar@nus.edu.sg

1 Department of Biological Sciences, National University of Singapore, 14 Science Drive 4, Singapore 117543, Singapore

2 Department of Biochemistry, National University of Singapore, 28 Medical Drive, Singapore 117546, Singapore

3 Department of Pharmacology, Yong Loo Lin School of Medicine, National University of Singapore, 16 Medical Drive, Singapore 117600, Singapore

4 Department of Biochemistry and Molecular Biology, Virginia Commonwealth University, 1101 E Marshall Street, Richmond, VA 23298, USA

genes. These genes, in turn, "restrict" viral replication and the subsequent establishment of a productive infection (or diseased state) [8–10]. Of the many interferon-stimulated genes expressed, Tripartite Motif proteins (TRIMs) have received significant attention as antiviral restriction factors [11]. Many TRIM proteins exert indirect inhibition by modulating interferon signalling in response to highly divergent viral infections, whereas others function by directly interacting with and inducing destruction of viral RNA or proteins [11]. Indeed, various studies have reported TRIM-mediated restriction of numerous arthropod-borne, positive-sense RNA viruses in addition to DENV, including Zika virus (ZIKV), West Nile virus (WNV), Japanese encephalitis virus (JEV), Yellow fever virus (YFV), Hepatitis C virus (HCV), and Tick-borne encephalitis virus (TBEV) [12–17].

Despite utilizing divergent antiviral mechanisms, TRIM family proteins are characterized by a conserved N-terminal tripartite motif comprising of the catalytic RING domain, one or two B-box domains, and coiled-coil (CC) domain which mediates TRIM dimerization, followed by a variable C-terminal domain which mediates interaction with target substrates [18]. Based on the C-terminal domain, TRIMs have been classified into 11 subfamilies with the largest C-IV subfamily characterized by the SPRY/B30.2 (PRY–SPRY) domain at the C-terminus being the largest [19].

The non-structural NS proteins are critical for viral replication and subverting the host antiviral response, and this is common to numerous flaviviruses [2]. The host counters this viral attack through the action of TRIMs as E3 ligases, which ubiquitinate and destroy the NS proteins [20]. Previous work has shown that TRIM52 interacts with and ubiquitinates the JEV NS2A protein, and that the C-terminal SPRY domain of TRIM14 interacts with the NS5A protein of HCV to mediate its ubiquitination [13, 14]. This ubiquitination function is similarly indispensable against a range of other viruses [21, 22]: the zinc-finger antiviral protein (ZAP) requires the E3-ligase activity of TRIM25 to restrict alphavirus Sindbis virus (SINV) in the host cell [21], and the in vivo replication of Influenza, a negative-sense RNA virus, is inhibited by TRIM56 via its C-terminal domain in a non-degradative manner [22].

Specifically, TRIMs have been shown to impede viral entry and inhibit viral transcription, replication, and spread within the host [23]. Understanding the specific roles of TRIM proteins as viral restriction factors will help to elucidate the antiviral mechanisms employed by hosts, as well as aid in the development of antiviral therapeutics.

In 2018, Wang and colleagues [16] identified the role for host TRIM69 in restricting DENV-2 replication by binding to and inducing the polyubiquitination-dependent proteasomal degradation of the NS3 protein [16]. However, the molecular determinants governing this interaction are still unknown. To this end, we investigated the interactions of human TRIM69 and the protease domain of DENV-2 NS2B–NS3 and mapped the binding regions. We found that the protease domain (NS3Δpro) of full-length NS3 was sufficient to interact with TRIM69 for polyubiquitination. We identified three regions on human TRIM69 spanning residues $Leu181^{T}$–$His199^{T}$, $Thr223^{T}$–$Glu234^{T}$ and $Ser398^{T}$–$Gly412^{T}$ that reside in the CC and PRY–SPRY domain as interaction sites for the NS3 protease (^{T} indicates TRIM69 residues). Furthermore, we identified the TRIM69 interaction sites on NS3Δpro as $Tyr73^{N}$–$Val90^{N}$; $Trp139^{N}$–$Leu148^{N}$; $Leu150^{N}$–$Leu165^{N}$ and $Pro188^{N}$–$Leu199^{N}$; these regions are conserved across DENV serotypes (DENV-1, DENV-3, and DENV-4) as well as other flavivirus NS3 proteins (^{N} indicates NS protein residues). Collectively, our findings show that TRIM69 interacts with NS3 through multiple distinct domains and suggests that the host deploys TRIM69 as a pan-antiviral factor to limit flavivirus infections.

Results

Sequence analysis

TRIM69 consists of four domains: the canonical RING-, B-box, CC (forming the tripartite/RBCC domain at the N-terminus), and C-terminal PRY–SPRY (Fig. 1a). Sequence alignment and phylogenetic analysis of human TRIM69 against other human TRIMs suggest that TRIM22, TRIM21, and TRIM69 diverge from a common ancestor (Fig. 1b). Further sequence alignment of TRIM RING domain (Figure SF1) shows conservation of key residues in these conserved domains. The acidic residue (Glu10) located at the N-terminal region of the core TRIM25 RING region is critical for stabilization of the RING/E2~Ub arrangement for ubiquitin transfer [24, 25]. An equivalent Glu38 residue is present in TRIM69, suggesting a similar role for TRIM69 in ubiquitin transfer (Figure SF1). The C-terminal PRY–SPRY domain of TRIMs has conserved β-strands and aromatic amino acid residues (Figure SF2) and is involved in interaction with distinct target proteins [20]. The PRY–SPRY domain of TRIM69 targets viral protease NS3, and thus can inhibit viral replication and promote clearance of virus.

TRIM69 ubiquitinates DENV-2 NS2B–NS3Δpro

We purified the full-length human TRIM69 protein (1–500 aa) as a GST-tagged construct and found that it eluted predominantly as a dimer in size-exclusion chromatography (Figure SF3). However, the Dynamic Light Scattering

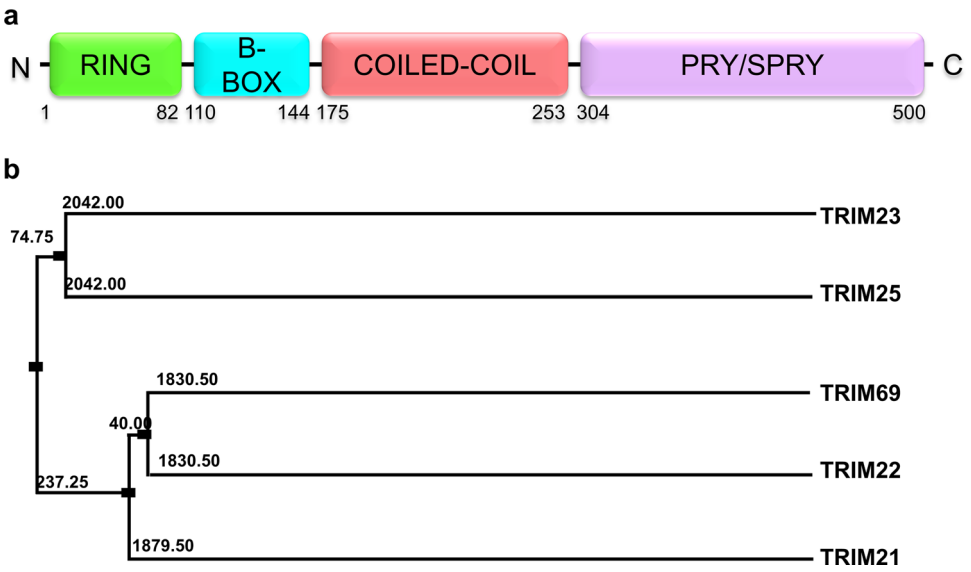

Fig. 1 Domain architecture and phylogenetic analysis of TRIM69 protein. **a** Schematic diagram of the domain organization of TRIM69 with the approximate residue boundaries. It contains a tripartite motif consisting of an N-terminal catalytic RING domain, a B-box domain, and coiled-coil (CC) domain, followed by a C-terminal SPRY domain. The RING domain contains two "zinc finger" motifs which exert TRIM's E3 ubiquitin ligase activity, the exact function of the B-box domain which also contains a "zinc finger" motif is unknown. The CC domain forms an antiparallel dimer and mediates homo- and hetero-dimerization of TRIMs, while the SPRY domain is involved in substrate recruitment. **b** Phylogenetic tree analysis for 5 major TRIM proteins, namely, TRIM21, TRIM22, TRIM23, TRIM25, and TRIM69 with antiflaviviral activity. The analysis shows that TRIM21, TRIM22, and TRIM69 descent from a common ancestor. Phylogram generated using Jalview [63]

(DLS) result indicates that TRIM69 forms a dimer of dimer (Figure SF3). The protein was unstable after cleaving the GST tag; therefore, all experiments were performed with GST–TRIM69.

The DENV-2 NS3 protease domain (NS3Δpro) requires the NS2B core region as a cofactor for its catalytic activity and stability [6]. Consequently, a His-tagged NS2B–NS3Δpro fusion construct was designed by connecting the core 18 residues of NS2B to the N-terminus of the NS3 protease domain (1–185 aa) through a flexible glycine-rich linker, as described previously by Luo et al., for DENV-4 full length NS3 [6]. This construct is hereafter referred to as "NS2B–NS3Δpro". The NS2B–NS3Δpro protein eluted as a monomer in gel filtration, and this was confirmed by dynamic light scattering (DLS) analysis (Figure SF4).

In Dengue virus suppression, TRIM69 interacts with and targets DENV NS3 for ubiquitination. Using ELISA, we assessed the interaction between purified DENV NS2B–NS3Δpro and TRIM69. We found that NS2B–NS3Δpro also interacts with TRIM69 (Fig. 2a), an observation hitherto not reported. An in vitro substrate ubiquitination assay was carried out using the recombinantly purified E1, E2, and E3 enzymes, and Ub and NS2B–NS3Δpro proteins (Figure SF5). We showed that TRIM69 as an E3 ligase can mediate ubiquitination of NS2B–NS3Δpro leading to the formation of polyubiquitinated products of NS2B–NS3Δpro (Fig. 2b). Thus, suggesting that TRIM69 likely affects the protease activity of NS2B–NS3Δpro, which, in turn, negatively impacts the viral replication process.

Characterization of TRIM69 and NS2B–NS3Δpro interactions using HDXMS

We next used amide hydrogen–deuterium exchange mass spectrometry (HDXMS) to identify the interaction interface between TRIM69 and NS2B–NS3Δpro, and to probe the accompanying changes in their conformational dynamics in a time-dependent manner [27–29].

Domain-specific conformational dynamics of TRIM69

Previous studies have reported the high-resolution crystal structures of TRIM69 RING (PDB: 4NQJ) and CC (PDB: 6YXE) domains, and described the dimerization of the TRIM69 RING domain during activation [24, 30]. However, these structures represent only a snapshot of the individual domains and not a complete picture of the intrinsic dynamics of the full-length TRIM69. Here, using full-length TRIM69, a total of 66 pepsin-cleaved peptide fragments were analysed, covering 87% of the primary sequence of the protein (Figure SF6).

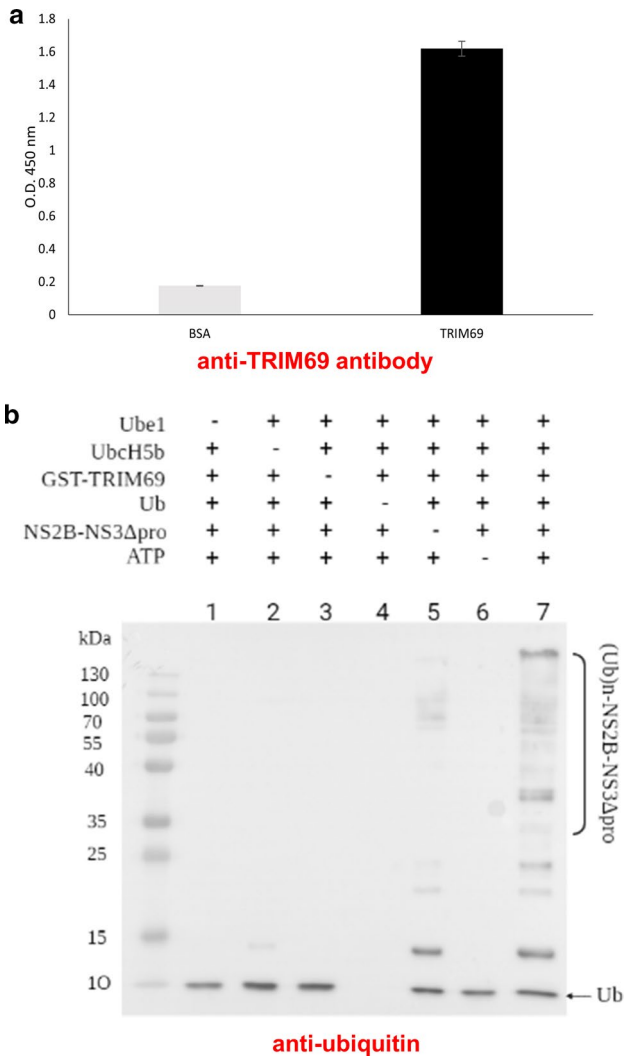

Fig. 2 ELISA confirms the interaction of TRIM69 with DENV NS2B–NS3 Protease. **a** Compared with BSA (grey bar) control, the NS2B–NS3Δpro showed direct interaction with TRIM69 (black bar) as observed by the increased absorbance at 450 nm, probed by anti-TRIM69 antibody. Here we show for the first time that the NS3 protease domain is alone sufficient for interaction with TRIM69. **b** TRIM69 mediates NS2B–NS3Δpro ubiquitination in vitro. Assay is carried out with recombinantly purified GST–TRIM69 (E3) in the presence (+) or absence (−) of each of the assay components (represented by lanes 1–7 in the blot), i.e., E1, E2 (UbcH5b), Ubiquitin, and ATP with NS2B–NS3Δpro as substrate. The reaction products were resolved on 12.5% SDS–PAGE gel and analysed by immunoblotting using anti-Ubiquitin antibody. NS2B–NS3Δpro (1–185 aa) ubiquitination was only observed in lane 7 in the presence of all the ubiquitination components, while partial TRIM69 autoubiquitination activity can be seen in lane 5

The HDXMS results revealed TRIM69 to be a highly dynamic protein, with an average protein-wide relative deuterium uptake (RFU) of ~0.4–0.5 across various peptides (Fig. 3a, ST1). A time-dependent increase in deuterium uptake was observed across most regions, with a short labelling time (1 min) indicative of low intrinsic dynamics, and a longer labelling time (10, 100 min) of high intrinsic dynamics. As expected, peptides spanning the dimer interface across the RING and CC domains showed relatively lower deuterium uptake (Fig. 3a, red and blue boxes) as compared with other regions. These domain-specific changes in the inherent dynamics of the anti-parallel TRIM69 dimer were reflected by mapping the RFU values onto a full-length model of TRIM69 (Fig. 3b); this model was predicted by AlphaFold2 (AF-Q86TW6-F1), which showed similarity to the high-resolution structures of individual domains of TRIM69 [24, 30, 31].

Conformational dynamics of NS2B–NS3Δpro

We next determined the inherent dynamics of DENV NS2B–NS3Δpro. Considering that the in vitro ubiquitination assays that were performed at 37 °C, the HDXMS experiments were also conducted at this temperature. We analysed a total of 75 peptides spanning > 93% of the amino acid sequence of NS2B–NS3Δpro (Figures SF7, ST2). A protein-wide profile of NS2B–NS3Δpro alone revealed protein-specific RFU, wherein peptides spanning His-NS2B (residues 1–70, pink box Fig. 3c) showed high RFU values (~0.4–0.6) at all labelling timeframes, as compared with the time-dependent increases in deuterium uptake observed for the NS3Δpro segment (green box, Fig. 3c). These conformational changes are better depicted by the heatmap of RFU values mapped onto a crystal structure (PDB ID: 2FOM) of a deletion construct (residues 48–220) of NS2B–NS3Δpro in Fig. 3d [32]. Peptides spanning the N-terminal and C-terminal residues of NS3 had the greatest deuterium uptake, suggesting these regions to be unstructured and highly dynamic, and, therefore, disordered in the crystal structures (PDB 2FOM and 6MO0). Heat maps of peptides spanning the central region of NS2B–NS3Δpro also showed time-dependent conformational changes and revealed large-scale domain movement (Fig. 3b). These loci- and domain-specific deuterium exchange values indicate that NS2B–NS3Δpro exhibits protein-specific inherent dynamic propensities in solution.

NS2B–NS3Δpro binding leads to conformational dynamics of TRIM69

Next, we sought to monitor the conformational changes accompanying TRIM69:NS2B–NS3Δpro complex formation. HDXMS experiments were performed with equimolar concentrations of TRIM69 and NS2B–NS3Δpro to stabilize the interaction. First, we examined the binding of NS2B–NS3Δpro to TRIM69 and observed the changes in deuterium exchange values of peptides spanning TRIM69. Comparing deuterium exchange values of TRIM69 in the presence or absence of NS2B–NS3Δpro, we observed that most peptides showed an overall decrease in deuterium

exchange (blue boxes, Fig. 4a, Table ST3). These results indicate that NS2B–NS3Δpro binding leads to a global reduction in the conformational dynamics of TRIM69. A "difference map" was generated by mapping these differences in deuterium exchange values onto the structures of different domains of TRIM69 (Fig. 4b). Regions showing lower deuterium uptake (mapped in shades of blue) were primarily located to the RING and CC domains, suggesting that NS2B–NS3Δpro binding promotes and stabilizes the dimerization of TRIM69, which is essential for its catalytic activity.

Peptides spanning residues Leu181^{T}–Leu199^{T}, Thr223^{T}–Glu234^{T}, and Ser398^{T}–Gly412^{T} (^{T} indicates TRIM69 residues) of the TRIM69 CC and SPRY domains, showed significantly large-scale increases in deuterium exchange in the complex state (pink boxes, Fig. 4a; mapped in red, Fig. 4b). The increase in deuterium exchange across these regions of TRIM69 indicates greater conformational flexibility at these loci upon NS2B–NS3Δpro binding. The full-length structure of TRIM69 generated by Alphafold (Fig. 4b) shows that the C-terminal SPRY domain protrudes from the TRIM69 long axis formed by the elongated CC structure without steric clashing. In addition, the large-scale increases in deuterium exchange indicate that NS2B–NS3Δpro binding induces domain movement across the C-terminal SPRY domain, which is accompanied by localized, partial unfolding of the CC domain (Fig. 6).

TRIM69 interacts with specific residues of NS2B–NS3Δpro

In parallel, we probed the effects of TRIM69 on NS2B–NS3Δpro structure as the result of their interaction and determined the complementary interaction interface map. We compared the changes in deuterium exchange of the NS2B–NS3Δpro:TRIM69 complex with that of NS2B–NS3Δpro alone (Fig. 4c, Table ST4). We observed predominant conformational changes across the NS2B–NS3Δpro protein at the 10-min labelling timepoint. NS2B–NS3Δpro shows an inherently high dynamic propensity; yet binding to TRIM69 did not lead to stable changes at all timepoints.

Peptides spanning residues Ala31^{N}–Glu41^{N} of the NS2B protein, and peptides covering Ala120^{N}–Trp133^{N}, Trp139^{N}–Leu148^{N}, Leu150^{N}–Leu165^{N}, and Pro188^{N}–Leu199^{N} (^{N} indicates NS2/3 protein residues) of NS3Δpro all showed decreases in deuterium exchange (blue boxes, Fig. 4c). These differences were mapped onto the crystal structure of the deletion construct of the NS2B–NS3Δpro fusion protein (PDB ID: 2FOM). The difference map of the NS2B–NS3Δpro:TRIM69 complex showed that the decreased deuterium exchange is prominent towards the C-terminal end of NS2B–NS3Δpro protein (mapped in blue, Fig. 4d). These results highlight the regions of NS2B–NS3Δpro that interact with TRIM69 and suggest that TRIM69 reduces the conformational dynamics of NS2B–NS3 and promotes proteolytic processing of this viral protein.

We found high sequence conservation for DENV-2 NS3Δpro when compared with NS3 protease domain of other DENV serotypes. Notably, Lys104, which is targeted by TRIM69 for ubiquitination, is conserved among the serotypes (Fig. 5a) [16]. This suggests that TRIM69 may interact with and ubiquitinate the NS2B–NS3 protease from other DENV serotypes. Similarly, sequence comparison revealed conservation in the NS3Δpro regions targeted by TRIM69, in addition to Lys104, among other flaviviruses, such as ZIKV and WNV (Fig. 5b). From this analysis, we propose that TRIM69 likely exhibits pan-antiviral activity against human–pathogenic flaviviruses through its ubiquitination activity. However, further studies are warranted to confirm the role of TRIM69 on these flaviviruses.

HDXMS reveals interaction interface of TRIM69:NS2B–NS3Δpro complex

We observed significant conformational dynamics for TRIM69 and NS2B–NS3Δpro at various regions. For TRIM69, decreased deuterium exchange was observed throughout the protein, with large-magnitude differences observed for the CC domain. Upon closer examination of the mass spectra of selected peptides of TRIM69, we observed characteristic mass spectral broadening of the isotopic distribution for peptides spanning the CC dimerization interface (Fig. 4a, pink boxes). Besides, the helical segments flanking the CC domain perpendicular to the short α-helices (peptide 126–141; B-box) showed increased deuterium exchange in the complex. These HDXMS results indicate that NS2B–NS3Δpro binding leads to reduced dynamics of TRIM69, wherein NS2B–NS3Δpro binds and promotes formation of higher order (tetrameric) oligomers of TRIM69 and mediates stable complex formation. Based on our observations and combined with previous predictions [24, 35], we propose a model for TRIM69:NS2B–NS3Δpro complex formation (Fig. 6). This complex mediates efficient NS2B–NS3Δpro substrate ubiquitination. In the complex the RING domains undergo juxtaposition and promote TRIM69 dimerization, with the SPRY domain binding to and stabilizing the interaction with the substrate, NS2B–NS3Δpro.

When in complex with TRIM69, we noted significant changes in deuterium exchange in NS2B–NS3Δpro for peptides that spanned the key residues of the NS3 protein. Superimposition of the two difference maps of TRIM69 and NS2B–NS3Δpro indicated that two molecules of NS2B–NS3Δpro become docked between the N-terminal

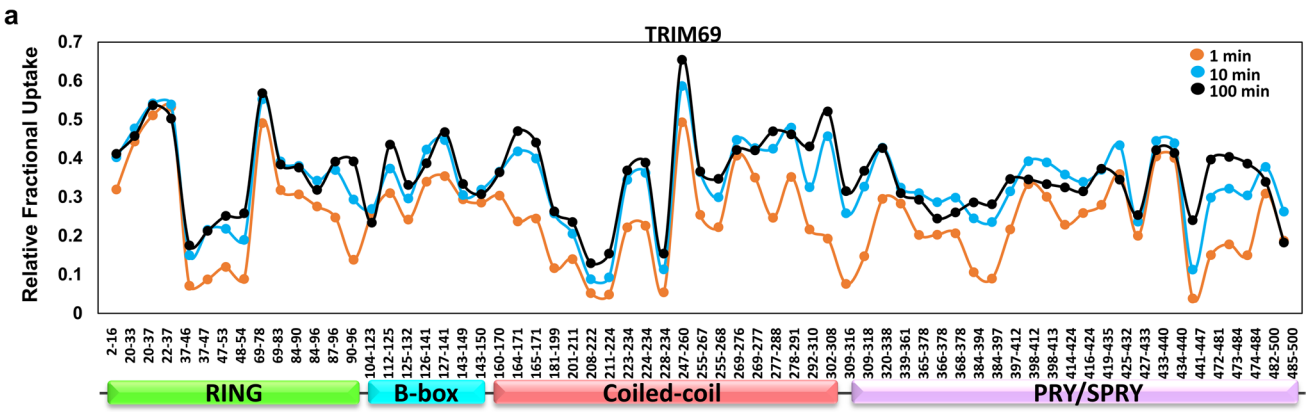
a
TRIM69
Relative Fractional Uptake
1 min
10 min
100 min
RING
B-box
Coiled-coil
PRY/SPRY

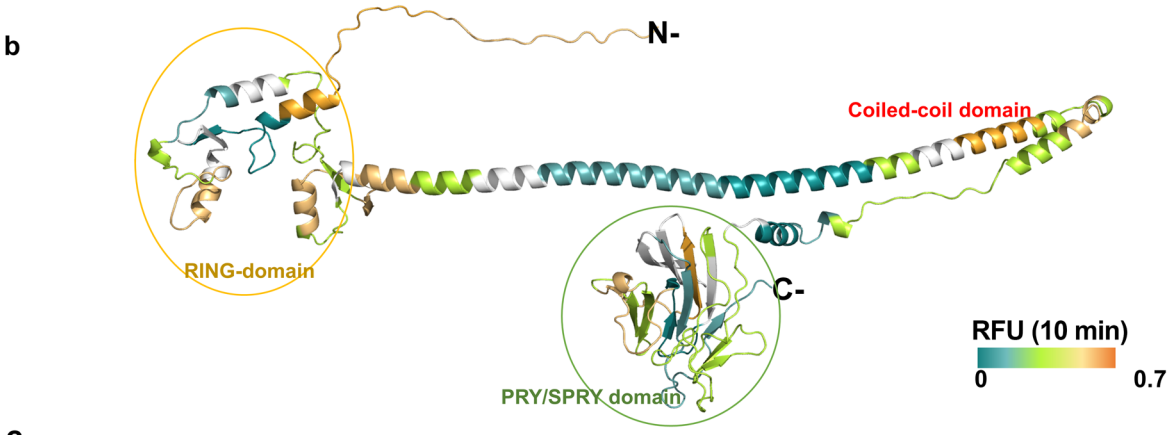
b
N-
Coiled-coil domain
RING-domain
C-
PRY/SPRY domain
RFU (10 min)
0
0.7

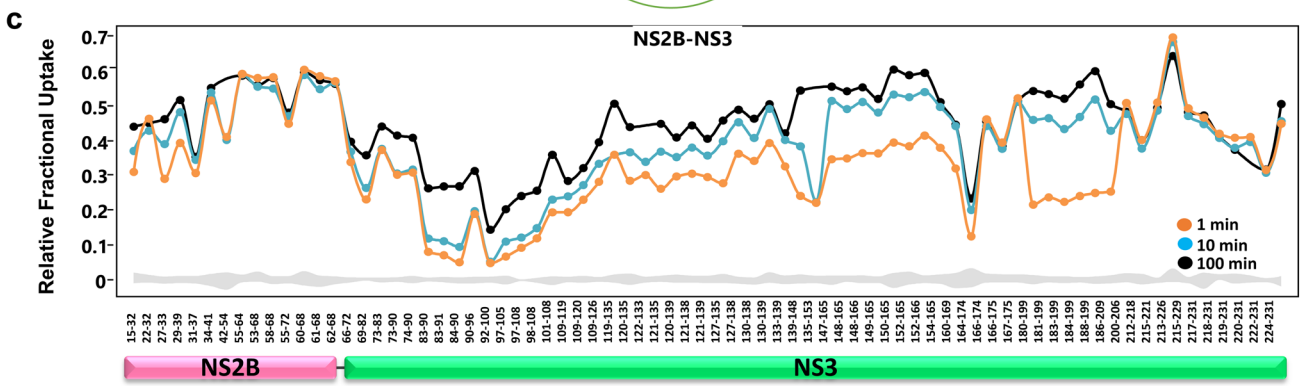
c
NS2B-NS3
Relative Fractional Uptake
1 min
10 min
100 min
NS2B
NS3

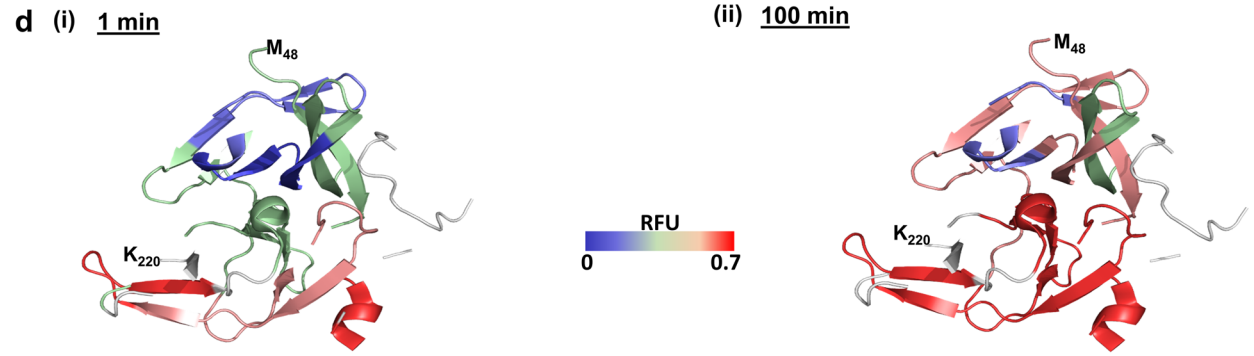
d (i) 1 min
(ii) 100 min
M48
K220
RFU
0
0.7

◂**Fig. 3** Intrinsic dynamics of TRIM69 and NS2B–NS3. Plot of relative fractional uptake (RFU, *y*-axis) of free TRIM69 (**a**) and NS2B–NS3Δpro (**c**) proteins for each pepsin digested fragment listed from N-to-C-terminus (*x*-axis) at three labeling times as indicated. Each dot represents each peptide with their residue numbers indicated as per the domain organization of TRIM69 (**a**) and NS2B–NS3 (**c**). **b** RFU values (10 min labeling time) are mapped onto a model of full-length TRIM69 (AF-Q86TW6-F1, generated from AlphaFold2) shown in cartoon representation and colored as indicated. **d** RFU values at 1 min (**d i**) and 100 min (**d ii**) labeling timepoints are mapped on to the high-resolution structure of deletion construct of NS2B–NS3Δpro (PDB:2FOM) monomer and indicated in cartoon representation. N- (M48) and C- (K220) residues of the structure are indicated for reference

RING and C-terminal SPRY domains flanking the central CC domain of a dimeric TRIM69, yielding a 2:2 stoichiometric interaction.

Discussion

The human immune system employs different mechanisms to prevent viral infection and pathogenesis. A key strategy is to curb viral replication via the actions of the host's E3 ligases, which ubiquitinate crucial viral proteins and target them for proteasomal degradation. Members of the Flaviviridae RNA virus family, including DENV, possess unique strategies to not only promote their replication in the host but also control the host's intrinsic immune response to prevent viral clearance. In particular, the DENV NS3, cleaves viral polyproteins to generate viral protein products, while it simultaneously suppresses the immune response by inhibiting Interferon α/β (IFN-α/β) induction [36, 37]. Wang et al., reported that human E3 ligase TRIM69 ubiquitinates DENV-2 NS3, thereby supressing the viral replication process [16, 38]. Ubiquitination of DENV NS2B/3 by TRIM69 for proteasomal degradation is the essential regulatory element of innate antiviral responses [11, 20, 23]. Although several TRIM protein interactions and the ubiquitination of several substrate NS proteins were reported [13, 14, 21, 22], the interaction interface region between TRIM and NS proteins, the requirement of minimum region of the substrate for ubiquitination were not known.

The mapping of interacting regions in the current study uncovers how TRIM69 recognizes and abrogates NS2B/NS3 activity. We characterized the interactions between human TRIM69 and the DENV-2 NS2B–NS3 protease. Our western blot analysis of the NS2B–NS3Δpro (1–185 aa) ubiquitination reaction in the presence of TRIM69 as E3 ligase confirmed that the NS3 protease domain is ubiquitinated, which marks the NS3 for clearance by the host proteasomal machinery (Fig. 2b). Using HDXMS analysis, we identified the interacting interface between these two proteins. Our domain mapping analysis reveals that both the CC and SPRY domains bind to NS3 (Fig. 4b). Three peptides situated within the CC and SPRY domains of TRIM69—Leu181^{T}–His199^{T}, Thr223^{T}–Glu234^{T}, Ser398^{T}–Gly412^{T}—interact with NS2B–NS3. From our results, we suggest that the NS3 protease domain alone is sufficient to act as target for TRIM69-mediated ubiquitin-dependent proteasomal degradation of the NS2B–NS3 protease complex.

TRIM69 binds to the C-terminus of the NS2B–NS3 protease complex. These interaction sites are key to active (closed) or inactive (open) conformations of NS2B relative to NS3Δpro. Our HDXMS results highlight that TRIM69 binding manifests significant conformational changes in the NS2B–NS3 protease, perhaps priming it for proteasomal degradation. A previous study reported that Lys104 (Lys154 in our fusion construct) acts as the ubiquitination site on NS3 [16]. The current data shows that the Lys104^{N} side chain protrudes away from the NS3 interaction interface (residues Trp139^{N}–Leu148^{N}) (Fig. 4c) with TRIM69, emphasizing the functional relevance of this interface in efficient NS3 ubiquitination. Sequence alignment reveals that these regions are well conserved across the DENV serotypes (DENV-1, DENV-3, and DENV-4), suggesting that TRIM69 might also target other DENV serotypes and play a pan-antiviral role against dengue virus infection. Moreover, we note high sequence conservation among the flavivirus NS3 proteins, including conservation of Lys104, which is essential for ubiquitination (Fig. 5A).

Based on the C-terminal PRY–SPRY domain structure, the TRIM69, TRIM21 and TRIM22 are classified as the Class-IV subfamily. Several Class-IV family TRIMs act as antiviral restriction factors against diverse families of viruses by directly targeting of the viral proteins (Table ST5). The TRIM-mediated resistance to viruses can be attributed to their conserved, multidomain composition. The RING domain confers E3 ligase activity [39–41], the B-box and CC-domains mediate higher order oligomerization (including dimerization) of TRIMs, which define the spatial organization of the RING and C-terminal SPRY [24, 33, 42–44], while the B30.2/SPRY domain mediates interaction with target substrates [18]. TRIM69 forms an antiparallel dimer in solution primarily due to self-association through its CC domain, which positions the RING domain at opposite ends of the dimer [33]. Multiple high-resolution structures of NS2B–NS3Δpro (PDB: 6MO0, 2FOM) show that it exists as a monomer [32, 34].

Molecular insights into the mechanism of action of some TRIM proteins have been investigated to identify the determinants for their restriction specificity [11, 12, 24]. In most cases, the SPRY domain mediates their interaction with the viral protein. Previous studies have shown that the TRIM21 interacts with the Fc segment of IgG, mediating an antiviral response to antibody opsonized adenovirus and targets the virus for proteasomal degradation [26]. Deletion mutant

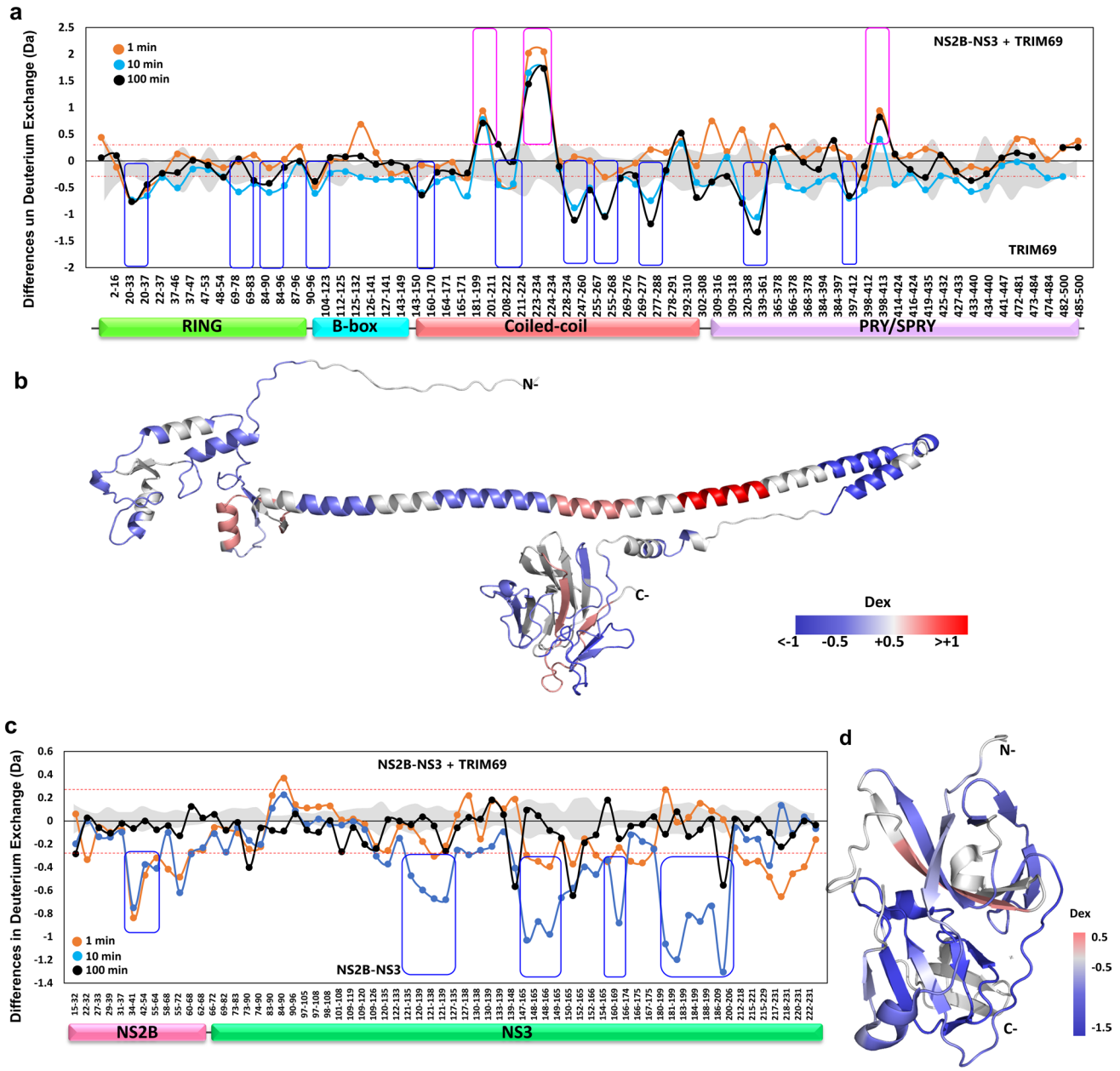

Fig. 4 HDXMS reveals conformational dynamics of NS2B–NS3 and TRIM69. Plots showing the differences in deuterium exchange values (*y*-axis) between TRIM69:NS2B–NS3 complex with free TRIM69 protein (**a**) and free NS2B–NS3 proteins (**c**) at different labeling times (1, 10, 100 min) for various pepsin-digested fragments listed from N-to-C-terminus (*x*-axis). ±0.3 Da is considered as significance threshold cutoff indicated by red-dashed lines and standard deviation is in gray. Positive differences indicate increased deuterium exchange (pink boxes) and negative values indicate decreased (blue boxes) deuterium exchange in TRIM69:NS2B–NS3Δpro complex. Blue boxes highlight peptides showing significant 'protection' against deuterium uptake in the peptides in TRIM69:NS2B–NS3Δpro complex. Differences at 10 min labeling time are mapped on to predicted model of **b** TRIM69 (AF-Q86TW6-F1) and **d** NS2B–NS3Δpro monomer (PDB: 2FOM), shown in cartoon representation as per key

analysis showed that the SPRY domain of TRIM14 interacts with IAV nucleoprotein (NP) and HBV HBx protein and leads to their degradation [45, 46]. Similarly, the SPRY domain of TRIM41 is sufficient for interaction with Enh I and Enh II proteins of HBV and the NP protein of IAV (Table ST5) [47, 48]. However, viral restriction requires RING E3 activity for efficient clearance of the protein by the ubiquitin–proteasome pathway [47–50]. These studies show that the host deploys multiple TRIM proteins, which might act in unison to effectively inhibit the viral lifecycle. In addition, certain TRIMs restrict viruses from multiple families, thus acting as a pan-antiviral, as exemplified by

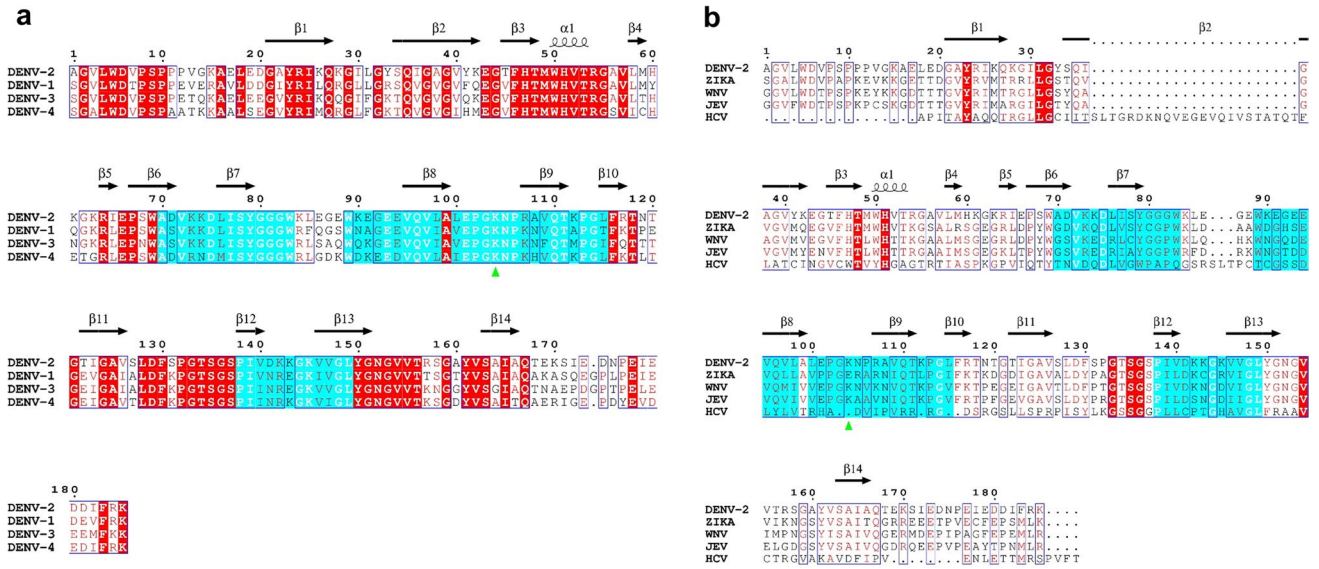

Fig. 5 Multiple Sequence alignment of DENV-2 NS3 protease with the protease domain from other DENV serotypes as well as related flaviviruses infecting humans. **a** Sequence alignment of NS3 protease domain (residues 1 to 185) from DENV-2 with the protease domain from other DENV serotypes. **b** Sequence alignment of DENV-2 NS3pro with NS3pro domain of other flaviviruses, such as ZIKV, WNV, JEV, and HCV. The peptide fragments from DENV-2 NS3 protease that mediate interaction with TRIM69 are highlighted in blue. Lys104 which is targeted by TRIM69 for ubiquitination is indicated with a green triangle and conserved across the DENV serotypes, WNV, and JEV. Columns are framed in blue for residues with greater than 70% similarity based on their physico-chemical properties. Residues are represented with single letter amino acid code, with identical residues indicated in white font and boxed in red, while identical are indicated in red font. Secondary structure elements are displayed above the protein sequence blocks. Alignments were generated using Clustal Omega and ESPript [64, 65]

TRIM22. The antiviral activity of TRIM22 depends on its RING E3 ligase activity varies depending on the virus [51]. The E3 ligase activity of TRIM22 RING domain is required for inhibition of HIV GAG [51], HCV NS5A [15], IAV NP [41], HBV core promoter (CP) [40], and EMCV $3C^{PRO}$ proteins, while its NLS (nuclear localization signal) and SPRY domain is sufficient to curtail PRRSV replication [15, 50–52]. On the other hand, certain TRIMs block viruses in a species or family specific manner. TRIM5α, the best characterized TRIM so far, acts as an antiviral factor against retroviruses. Its RBCC motif mediates higher order oligomerization, which supports multivalent interactions with the viral capsid lattice, while the SPRY domain facilitates viral restriction. In addition, species specific retroviral restriction by TRIM5α has been observed with the rhesus monkey orthologue of TRIM5α (rhTRIM5α) being able to antagonize HIV-1, while the human TRIM5α is ineffective against HIV [43, 53–56]. These studies help to understand the molecular interface of host–pathogen interactions that helps identify their role in the innate immune response.

The above studies, however, do not define the finer details molecular interactions between TRIMs and the viral proteins and shed light on the overall changes in the TRIM protein which facilitates efficient interaction targeting the viral protein. As such, the current report represents the first study that describes the protein surfaces that are involved in the interaction between TRIM69 and viral protein NS2B–NS3. Furthermore, our study elucidates the molecular mechanism and overall dynamics of host TRIM69–viral protein interactions, which might target not only one, but rather several members of the flaviviridae family. Collectively, our study points toward TRIM69 as a host factor with antiviral activity against flaviviruses. These findings will aid in future investigations for the development of drug targets against NS2B–NS3 proteases.

Materials and methods

Recombinant protein cloning, expression, and purification

The gene construct encoding DENV-2 NGC (GenBank M29095) NS2B–NS3 sequence was designed by linking the core fragment spanning residues 43–66 from NS2B linked to full length NS3 (residues 1–618) via a Gly–Ser–Gly linker, as described previously [6]. The gene was codon optimized and synthesized into pET-32b plasmid by GenScript (Piscataway). To generate the NS2B–NS3Δpro construct the region coding for NS2B–NS3 protease domain was amplified by PCR using forward primer (5′-GCCGGATCCCTC GAGGCTGATTTG GAACTG-3′) and reverse primer

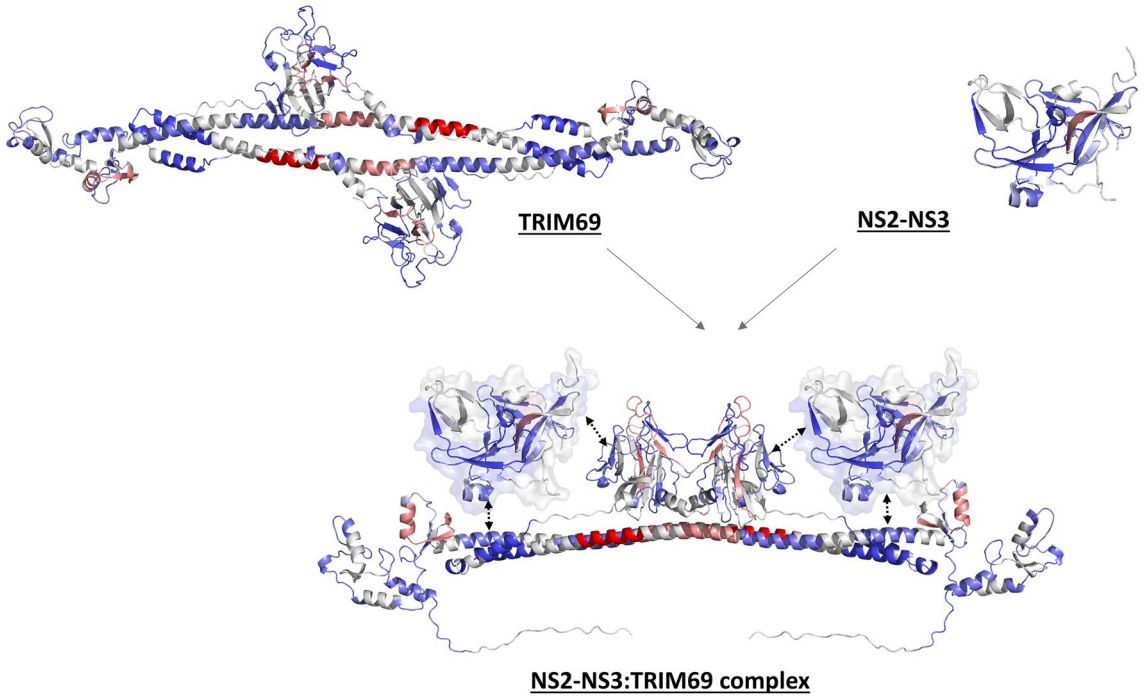

Fig. 6 Model of interaction of TRIM69 and NS2B–NS3Δpro. HDXMS data revealed various peptides showing protection against deuterium exchange in TRIM69 and NS2B–NS3Δpro protein during their complex formation. The differences in deuterium exchange values were mapped onto structures of TRIM69 (AF-Q86TW6-F1) and NS2B–NS3Δpro (2FOM), shown in cartoon representation. Difference map at 10 min of deuterium labelling is shown for transverse orientation of dimeric TRIM69 (dimer, left) and NS2B–NS3Δpro (monomer, right). Based on the residues showing protection, an interaction model is shown in 2:2 stoichiometry ratio of TRIM69:NS2B–NS3Δpro, with the predicted regions of interaction indicated by double-headed arrows

(5′-AAAAAGCTTTTACTT TCGAAAGATGTCATC-3′). The amplified product was digested with BamHI and HindIII restriction enzymes and cloned into similarly digested pET-M vector (a modified pET-32a vector designed in our laboratory by removing the thioredoxin tag) using T4 ligase (Roche). The expression construct codes for a N-terminal hexa-histidine tag fused to N-terminus of NS2B–NS3Pro. The genes coding for full-length human TRIM69, ubiquitin (Ub), and UbcH5b (E2) were purchased from GenScript (USA) in pGEX-6P-1 vector (GE healthcare). The plasmid coding for the His-tagged Ube1 (34965, deposited by Cynthia Wolberger) was purchased from Addgene (Cambridge, MA, USA).

E. coli BL21(DE3) cells transformed with GST-fusion plasmids, while ultracompetent *E. coli* shuffle cells were used for expressing recombinant NS2B–NS3Δpro protein. Briefly, bacterial cells were cultured in LB medium supplemented with 100 µg/mL ampicillin and grown at 37 °C until the absorbance (600 nm) reached ~ 0.8, induced with 0.4 mM Isopropyl β-D-1-thiogalactopyranoside (IPTG) and shifted to 16 °C, overnight. Cells expressing TRIM69 and NS2B–NS3Δpro were supplemented with 60 µM $ZnCl_2$ solution as both proteins are zinc-binding proteins. Harvested cell pellets were resuspended in lysis buffer (50 mM Tris–Cl pH 7.5, 0.5 M NaCl, 5% glycerol, 3 mM DTT) supplemented with protease cocktail inhibitor tablet (Roche). The cells were lysed by sonication and clarified by centrifuged at 18,000 rpm for 30 min (Beckmann Coulter centrifuge JA-20 rotor) at 4 °C. The clarified supernatant was loaded onto Ni–NTA beads (Qiagen) or GST beads (Qiagen) pre-equilibrated with lysis buffer. The column was washed thrice with lysis buffer, supplemented with imidazole (10–50 mM) for Ni–NTA purification. The protein was eluted with lysis buffer supplemented with 500 mM Imidazole for His-NS2B–NS3Δpro and Ube1, while 50 mM reduced glutathione was used to elute TRIM69. For GST-tagged Ub and UbcH5b proteins, on-column GST-tag cleavage was performed (overnight at 4 °C) using PreScission Protease (GE Healthcare), prior to gel filtration chromatography. Proteins were further purified to homogeneity using gel filtration and ion-exchange chromatography using ÄKTA pure chromatography system (GE Healthcare) on a Superdex™ 200 10/300 GL (Analytical S200)/HiLoad™ 16/600 Superdex™ 200 pg/HiLoad™ 16/600 Superdex™ 75 pg in buffer (20 mM Tris 7.5/8.0, 0.15 M NaCl, 5% glycerol, 1 mM DTT). Followed by Mono Q™ 5/50 GL anion-exchange chromatography to remove any impurities. Eluted protein was concentrated

using Amicon centrifugal filters and quantified using Nanodrop spectrophotometer. All the dynamic light scattering studies were carried out on a DynaPro NanoStar Dynamic Light Scattering instrument (Wyatt Technology Corporation, CA, USA).

Enzyme linked immunosorbent assay (ELISA)

ELISA assay was carried out between TRIM69 and NS2B–NS3Δpro proteins. 5 µg of NS2B–NS3Δpro protein or BSA as control in coating buffer was coated on 96-well plates (Thermo Fisher Scientific, MA, USA) overnight at 4 °C. The plates were washed twice with PBS and blocked with 1% BSA in PBS + 0.01% Tween-20) for 2 h at room temperature. Proteins were bound with 100 µL of TRIM69 (1 µg) at 37 °C for 1 h. Plate was washed three times to remove unbound proteins, and incubated with 100 µL of 1 µg/mL monoclonal mouse anti-GST (sc-53909; Santa Cruz Biotechnology, Santa Cruz, CA, USA) or polyclonal rabbit anti-Ubiquitin (sc-9133; Santa Cruz Biotechnology, Santa Cruz, CA, USA) as primary antibody for 2 h at room temperature. To remove traces of unbound antibody, the plate was washed three times with PBST, and incubated with 100 µL of 1:5000 dilution goat anti-mouse $F(ab')_2$–HRP-conjugated (sc-3697; Santa Cruz Biotechnology, Santa Cruz, CA, USA) or goat anti-rabbit HRP-conjugated (A120-101P; BETHYL laboratories, Inc, TX, USA) as secondary antibody. Plates were washed and then visualized by adding 80 µL of substrate TMB (3,3′,5,5′-tetramethylbenzidine) and the reaction stopped with 1 M HCl. Absorbance values at 450 nM were measured on Tecan Infinite 200 PRO multimode plate reader (Tecan Group Ltd., Switzerland).

In vitro ubiquitination assays

To assess the activity, ubiquitination assay was performed. Each reaction consisted of 0.05 µM E1 (Ube1), 1 µM E2 (UbcH5b), 2 µM TRIM69 as E3 ligase, and 20 µM WT Ubiquitin kept at 37 °C overnight in a reaction buffer (50 mM HEPES, pH 7.5, 100 mM NaCl, 10 mM $MgCl_2$, 5 mM ATP and 1 mM DTT) for autoubiquitination. Subsequently 2 µM His-NS2B–NS3Δpro was added to the reaction mixture for substrate ubiquitination. To quench the reaction, 6× SDS loading dye was added and the samples were subjected to boiling for 10 min at 95 °C. Denaturing gel electrophoresis was performed to assess the samples, followed by western blotting to probe the proteins using anti-ubiquitin antibody (1:2000 dilution). The western-blot membrane was washed with 1× TBS (with 0.05% Tween-20), and incubated with horseradish peroxidase (HRP)-conjugated goat anti-mouse as secondary antibody in a 1:10,000 dilution. Immobilon® Crecendo Western HRP substrate (Millipore, Merck) was used to detect the antibody-bound protein bands following the manufacture's protocol. The bands were visualized with GeneSys figure acquisition software with Syngene PXI multi-application Gel Imaging system (Cambridge, UK).

Hydrogen–deuterium exchange (HDXMS) of TRIM69–NS3 interaction

Conformational changes accompanying the protein–protein interaction of TRIM69 with NS2B–NS3Δpro were determined by HDXMS. HDXMS analysis was carried out for free TRIM69, free NS2–NS3Δpro and TRIM69:NS2–NS3Δpro complex. For each hydrogen–deuterium exchange labeling reaction ~ 75 pmol of the protein was diluted in deuterated buffer (50 mM HEPES pH 7.5, 100 mM NaCl) to a final 90% D_2O concentration. For HDXMS of free proteins, 3 µL of 1.5 mg/mL of TRIM69 and 0.25 µL of 7 mg/mL of NS2–NS3Δpro were used. For HDXMS of complex, 3 µL of 1.5 mg/mL of TRIM69 and 0.25 µL of 3.5 mg/mL of NS2–NS3Δpro were mixed as 2:2 stoichiometric ratio and incubated for 15 min before deuterium labeling reaction. Deuterium labeling for the three conditions was carried out for 1-, 10-, and 100-min timepoints at 37 °C. The exchange reaction was stopped by lowering the pH to ~ 2.6 and temperature to 0 °C by addition of chilled quench solution (0.5 M guanidinium hydrochloride, 10 mM Dithiothreitol, trifluoroacetic acid). Non-deuterated control experiments of TRIM69 and NS2–NS3Δpro alone were also carried out by diluting the samples in aqueous buffer, followed by quench solution. Non-deuterated reactions are references to determine the masses of individual peptides.

The quenched samples were incubated on ice (0 °C) for 15 s and then injected into HDX sample manager (Waters, USA) for pepsin digestion. Samples were subjected to non-specific proteolytic cleavage for 3 min by loading onto immobilized pepsin cartridge (Enzymate™, Waters, USA) maintained at 12 °C [57]. Quenched samples were pumped at 100 µl/min flow of 0.1% formic acid in LC–MS grade water (Merck KGA, Germany) by auxiliary sample manager (nanoACQUITY™, Waters, USA). Next, the digested pepsin-cleaved fragments ("peptides") were then trapped onto VanGuard C18 pre-column followed by reverse-phase chromatography using ACQUITY UPLC BEH C18 (1.7 µm, 1.0 × 100 mm) column. To minimize deuterium–hydrogen back exchange, a 'near-zero degree' ultra-performance liquid chromatography ("UPLC") was carried out by maintaining the column at 0–3 °C temperature [58]. Peptides were eluted using a 10 min long 8–40%

gradient of increasing concentration of solvent B (0.1% formic acid in acetonitrile) and decreasing concentration of solvent A (0.1% formic acid in water), pumped at 40 µl/min by nanoACQUITY™ binary solvent manager. The peptides eluted were then subjected to mass analysis by injecting onto a coupled high resolution Synapt G2-Si mass spectrometer (Waters, Manchester, UK).

Mass spectrometry data acquisition and HDXMS data analysis

Mass spectrometry data for each sample was acquired for 10 min with mass spectrometer operated in ion-mobility HDMS^E mode [28, 58–60]. Mass spectra of non-deuterated controls were used for peak identification and peptide matching using ProteinLynx Global Server v3.0.1 software (Waters, Milford, MA, USA) against individual databases consisting amino acid sequences of TRIM69 (UniProt ID: Q86WT6) and NS2B–NS3Δpro (UniProt ID: Q91H74). A list of identified peptides was generated from three different replicates, which was then loaded onto a semi-automated software DynamX v3.0 (Waters, Milford, MA, USA) for analysis of deuteration of various peptides. Amount of deuterium incorporated was estimated as 'centroid' values and estimated as the mass differences of deuterated peptide and non-deuterated peptide [60]. Relative deuterium uptake (RFU) of each peptide was then calculated as the ratio of number of deuterons incorporated by the peptide to the maximum number of exchangeable amides available for the peptide. All values reported are an average of biological replicates, each performed in three independent deuterium exchange reactions, and are not corrected for their back-exchange [60–62].

Supplementary Information The online version contains supplementary material available at https://doi.org/10.1007/s00018-022-04245-x.

Acknowledgements Authors thank Mr. Tan Ying Chong for his help in the protein purification. Bagga Tanaya is a graduate scholar in receipt of the graduate scholarship, National University Singapore.

Author contributions Conceptualization and study design were done by TB, KRM, NKT and JS. Protein purification and assay work was performed by TB. Mass spectrometry experiments were carried out by NKT. The first draft of manuscript was written by TB, NKT and JS. All authors read and approved the final version of the manuscript.

Funding This work was supported by the Ministry of Education, Singapore (MoE Tier 3, R154-000-697-112) and academic research fund (Tier 1, R154-000-C07-114) grants.

Data availability The data sets generated and analysed in the current study are available as supplementary tables. Any other data or materials will be made available upon request to the corresponding author(s).

Declarations

Conflict of interest The authors declare that they have no conflicts of interest.

Ethics approval Not applicable.

Consent to participate Not applicable.

Consent to publish Not applicable.

References

1. Bhatt S, Gething PW, Brady OJ et al (2013) The global distribution and burden of dengue. Nature 496(7446):504–507. https://doi.org/10.1038/nature12060
2. Fernandez-Garcia MD, Mazzon M, Jacobs M, Amara A (2009) Pathogenesis of flavivirus infections: using and abusing the host cell. Cell Host Microbe 5(4):318–328. https://doi.org/10.1016/j.chom.2009.04.001
3. Assenberg R, Mastrangelo E, Walter TS et al (2009) Crystal structure of a novel conformational state of the flavivirus NS3 protein: implications for polyprotein processing and viral replication. J Virol 83(24):12895–12906. https://doi.org/10.1128/jvi.00942-09
4. Falgout B, Pethel M, Zhang YM, Lai CJ (1991) Both nonstructural proteins NS2B and NS3 are required for the proteolytic processing of dengue virus nonstructural proteins. J Virol 65(5):2467–2475. https://doi.org/10.1128/jvi.65.5.2467-2475.1991
5. Bera AK, Kuhn RJ, Smith JL (2007) Functional characterization of cis and trans activity of the flavivirus NS2B-NS3 protease. J Biol Chem 282(17):12883–12892. https://doi.org/10.1074/jbc.M611318200
6. Luo D, Xu T, Hunke C, Grüber G, Vasudevan SG, Lescar J (2008) Crystal structure of the NS3 protease-helicase from dengue virus. J Virol 82(1):173–183. https://doi.org/10.1128/jvi.01788-07
7. Constant DA, Mateo R, Nagamine CM, Kirkegaard K (2018) Targeting intramolecular proteinase NS2B/3 cleavages for trans-dominant inhibition of dengue virus. Proc Natl Acad Sci USA 115(40):10136–10141. https://doi.org/10.1073/pnas.1805195115
8. Diamond MS, Roberts TG, Edgil D, Lu B, Ernst J, Harris E (2000) Modulation of dengue virus infection in human cells by alpha, beta, and gamma interferons. J Virol 74(11):4957–4966. https://doi.org/10.1128/jvi.74.11.4957-4966.2000
9. Shresta S, Kyle JL, Snider HM, Basavapatna M, Beatty PR, Harris E (2004) Interferon-dependent immunity is essential for resistance to primary dengue virus infection in mice, whereas T- and B-cell-dependent immunity are less critical. J Virol 78(6):2701–2710. https://doi.org/10.1128/jvi.78.6.2701-2710.2004
10. Tremblay N, Freppel W, Sow AA, Chatel-Chaix L (2019) The interplay between dengue virus and the human innate immune system: a game of hide and seek. Vaccines 7(4):145. https://doi.org/10.3390/vaccines7040145
11. Koepke L, Gack MU, Sparrer KM (2021) The antiviral activities of TRIM proteins. Curr Opin Microbiol 59:50–57. https://doi.org/10.1016/j.mib.2020.07.005
12. Liu B, Li NL, Wang J et al (2014) Overlapping and distinct molecular determinants dictating the antiviral activities of TRIM56 against flaviviruses and coronavirus. J Virol 88(23):13821–13835. https://doi.org/10.1128/jvi.02505-14
13. Fan W, Wu M, Qian S et al (2016) TRIM52 inhibits Japanese encephalitis virus replication by degrading the viral NS2A. Sci Rep 6:1–11. https://doi.org/10.1038/srep33698

14. Wang S, Chen Y, Li C et al (2016) TRIM14 inhibits hepatitis C virus infection by SPRY domain-dependent targeted degradation of the viral NS5A protein. Sci Rep 6:1–12. https://doi.org/10.1038/srep32336
15. Yang C, Zhao X, Sun D et al (2016) Interferon alpha (IFNα)-induced TRIM22 interrupts HCV replication by ubiquitinating NS5A. Cell Mol Immunol 13(1):94–102. https://doi.org/10.1038/cmi.2014.131
16. Wang K, Zou C, Wang X et al (2018) Interferon-stimulated TRIM69 interrupts dengue virus replication by ubiquitinating viral nonstructural protein 3. PLoS Pathog 14(8):1–24. https://doi.org/10.1371/journal.ppat.1007287
17. Wang J, Liu B, Wang N, Lee Y-M, Liu C, Li K (2011) TRIM56 is a virus- and interferon-inducible E3 ubiquitin ligase that restricts pestivirus infection. J Virol 85(8):3733–3745. https://doi.org/10.1128/jvi.02546-10
18. Meroni G, Diez-Roux G (2005) TRIM/RBCC, a novel class of "single protein RING finger" E3 ubiquitin ligases. BioEssays 27(11):1147–1157. https://doi.org/10.1002/bies.20304
19. Marín I (2012) Origin and diversification of TRIM ubiquitin ligases. PLoS One 7(11):e50030. https://doi.org/10.1371/journal.pone.0050030
20. van Tol S, Hage A, Giraldo MI, Bharaj P, Rajsbaum R (2017) The TRIMendous role of TRIMs in virus-host interactions. Vaccines 5(3):1–38. https://doi.org/10.3390/vaccines5030023
21. Li MMH, Lau Z, Cheung P et al (2017) TRIM25 enhances the antiviral action of zinc-finger antiviral protein (ZAP). PLoS Pathog 13(1):1–25. https://doi.org/10.1371/journal.ppat.1006145
22. Liu B, Li NL, Shen Y et al (2016) The C-terminal tail of TRIM56 dictates antiviral restriction of influenza A and B viruses by impeding viral RNA synthesis. J Virol 90(9):4369–4382. https://doi.org/10.1128/jvi.03172-15
23. Hage A, Rajsbaum R (2019) To TRIM or not to TRIM: the balance of host-virus interactions mediated by the ubiquitin system. J Gen Virol 100(12):1641–1662. https://doi.org/10.1099/jgv.0.001341
24. Koliopoulos MG, Esposito D, Christodoulou E, Taylor IA, Rittinger K (2016) Functional role of TRIM E3 ligase oligomerization and regulation of catalytic activity. EMBO J 35(11):1204–1218. https://doi.org/10.15252/embj.201593741
25. Sanchez JG, Chiang JJ, Sparrer KMJ et al (2017) Mechanism of TRIM25 catalytic activation in the antiviral RIG-I pathway. Physiol Behav 176(10):139–148. https://doi.org/10.1016/j.celrep.2016.06.070.Mechanism
26. Vaysburd M, Watkinson RE, Cooper H et al (2013) Intracellular antibody receptor TRIM21 prevents fatal viral infection. Proc Natl Acad Sci USA 110(30):12397–12401. https://doi.org/10.1073/pnas.1301918110
27. Konermann L, Pan J, Liu YH (2011) Hydrogen exchange mass spectrometry for studying protein structure and dynamics. Chem Soc Rev 40(3):1224–1234. https://doi.org/10.1039/c0cs00113a
28. Wales TE, Engen JR (2006) Hydrogen exchange mass spectrometry for the analysis of protein dynamics. Mass Spectrom Rev 25(1):158–170. https://doi.org/10.1002/mas.20064
29. Hodge EA, Benhaim MA, Lee KK (2020) Bridging protein structure, dynamics, and function using hydrogen/deuterium-exchange mass spectrometry. Protein Sci 29(4):843–855. https://doi.org/10.1002/pro.3790
30. Keown JR, Yang J, Black MM, Goldstone DC (2020) The RING domain of TRIM69 promotes higher-order assembly. Acta Crystallogr Sect D Struct Biol 76:954–961. https://doi.org/10.1107/S2059798320010499
31. Tunyasuvunakool K, Adler J, Wu Z et al (2021) Highly accurate protein structure prediction for the human proteome. Nature 596(7873):590–596. https://doi.org/10.1038/s41586-021-03828-1
32. Yao Y, Huo T, Lin YL et al (2019) Discovery, X-ray crystallography and antiviral activity of allosteric inhibitors of flavivirus NS2B-NS3 protease. J Am Chem Soc 141(17):6832–6836. https://doi.org/10.1021/jacs.9b02505
33. Li Y, Wu H, Wu W et al (2014) Structural insights into the TRIM family of ubiquitin E3 ligases. Cell Res 24(6):762–765. https://doi.org/10.1038/cr.2014.46
34. Erbel P, Schiering N, D'Arcy A et al (2006) Structural basis for the activation of flaviviral NS3 proteases from dengue and West Nile virus. Nat Struct Mol Biol 13(4):372–373. https://doi.org/10.1038/nsmb1073
35. Esposito D, Koliopoulos MG, Rittinger K (2017) Structural determinants of TRIM protein function. Biochem Soc Trans 45(1):183–191. https://doi.org/10.1042/BST20160325
36. Angleró-Rodríguez YI, Pantoja P, Sariol CA (2014) Dengue virus subverts the interferon induction pathway via NS2B/3 protease-IκB kinase ε interaction. Clin Vaccine Immunol 21(1):29–38. https://doi.org/10.1128/CVI.00500-13
37. Shin C, Choi D-S (2019) Essential roles for the non-canonical IκB kinases in linking inflammation to cancer, obesity, and diabetes. Cells 8(2):178. https://doi.org/10.3390/cells8020178
38. Han Y, Li R, Gao J, Miao S, Wang L (2012) Characterisation of human RING finger protein TRIM69, a novel testis E3 ubiquitin ligase and its subcellular localisation. Biochem Biophys Res Commun 429(1–2):6–11. https://doi.org/10.1016/j.bbrc.2012.10.109
39. Mu T, Zhao X, Zhu Y, Fan H, Tang H (2020) The E3 ubiquitin ligase TRIM21 promotes HBV DNA polymerase degradation. Viruses 12(3):346. https://doi.org/10.3390/v12030346
40. Gao B, Duan Z, Xu W, Xiong S (2009) Tripartite motif-containing 22 inhibits the activity of hepatitis B virus core promoter, which is dependent on nuclear-located RING domain. Hepatology 50(2):424–433. https://doi.org/10.1002/hep.23011
41. Di Pietro A, Kajaste-Rudnitski A, Oteiza A et al (2013) TRIM22 inhibits influenza A virus infection by targeting the viral nucleoprotein for degradation. J Virol 87(8):4523–4533. https://doi.org/10.1128/jvi.02548-12
42. Javanbakht H, Yuan W, Yeung DF et al (2006) Characterization of TRIM5α trimerization and its contribution to human immunodeficiency virus capsid binding. Virology 353(1):234–246. https://doi.org/10.1016/j.virol.2006.05.017
43. Li X, Sodroski J (2008) The TRIM5α B-Box 2 domain promotes cooperative binding to the retroviral capsid by mediating higher-order self-association. J Virol 82(23):11495–11502. https://doi.org/10.1128/jvi.01548-08
44. Goldstone DC, Walker PA, Calder LJ et al (2014) Structural studies of postentry restriction factors reveal antiparallel dimers that enable avid binding to the HIV-1 capsid lattice. Proc Natl Acad Sci USA 111(26):9609–9614. https://doi.org/10.1073/pnas.1402448111
45. Wu X, Wang J, Wang S et al (2019) Inhibition of influenza A virus replication by TRIM14 via its multifaceted protein-protein interaction with NP. Front Microbiol 10:1–14. https://doi.org/10.3389/fmicb.2019.00344
46. Tan G, Xu F, Song H et al (2018) Identification of TRIM14 as a type I IFN-stimulated gene controlling hepatitis B virus replication by targeting HBx. Front Immunol 9:1–14. https://doi.org/10.3389/fimmu.2018.01872
47. Zhang S, Guo JT, Wu JZ, Yang G (2013) Identification and characterization of multiple TRIM proteins that inhibit hepatitis B virus transcription. PLoS One 8:e70001
48. Patil G, Zhao M, Song K, Hao W, Bouchereau D, Wang L, Li S (2018) TRIM41-mediated ubiquitination of nucleoprotein limits influenza A virus infection. J Virol 92:e00905-18
49. McEwan WA, Tam JC, Watkinson RE, Bidgood SR et al (2013) Intracellular antibody-bound pathogens stimulate immune signaling via the Fc receptor TRIM21. Nat Immunol 14:327–336

50. Eldin P, Papon L, Oteiza A, Brocchi E, Lawson TG, Mechti N (2009) TRIM22 E3 ubiquitin ligase activity is required to mediate antiviral activity against encephalomyocarditis virus. J Gen Virol 90:536–545
51. Barr SD, Smiley JR, Bushman FD (2008) The interferon response inhibits HIV particle production by induction of TRIM22. PLoS Pathog 4:e1000007
52. Jing H, Tao R, Dong N, Cao S, Sun Y et al (2019) Nuclear localization signal in TRIM22 is essential for inhibition of type 2 porcine reproductive and respiratory syndrome virus replication in MARC-145 cells. Virus Genes 55:660–672
53. Morger D, Zosel F, Buhlmann M, Zuger S et al (2018) The threefold axis of the HIV-1 capsid lattice is the species-specific binding interface for TRIM5alpha. J Virol 92:e01541-17
54. Wagner JM, Christensen DE, Bhattacharya A et al (2018) General model for retroviral capsid pattern recognition by TRIM5 proteins. J Virol 92:e01563-17
55. Stremlau M, Owens CM, Perron MJ et al (2004) The cytoplasmic body component TRIM5alpha restricts HIV-1 infection in Old World monkeys. Nature 427:848–853
56. Ohkura S, Goldstone DC, Yap MW et al (2011) Novel escape mutants suggest an extensive TRIM5alpha binding site spanning the entire outer surface of the murine leukemia virus capsid protein. PLoS Pathog 7:e1002011
57. Hamuro Y, Coales SJ, Molnar KS, Tuske SJ, Morrow JA (2008) Specificity of immobilized porcine pepsin in H/D exchange compatible conditions. Rapid Commun Mass Spectrom 22:1041–1046
58. Wales TE, Fadgen KE, Gerhardt GC, Engen JR (2008) High-speed and high-resolution UPLC separation at zero degrees Celsius. Anal Chem 80:6815–6820. https://doi.org/10.1016/j.pestbp.2011.02.012
59. Raghuvamsi P, Tulsian N, Samsudin F et al (2021) SARS-CoV-2 S protein ACE2 interaction reveals novel allosteric targets. bioRxiv. https://doi.org/10.1101/2020.10.13.337212
60. Tulsian NK, Ghode A, Anand GS (2020) Adenylate control in cAMP signaling: implications for adaptation in signalosomes. Biochem J 477(16):2981–2998. https://doi.org/10.1042/BCJ20200435
61. Houde D, Berkowitz SA, Engen JR (2012) The utility of hydrogen/deuterium exchange mass spectrometry in biopharmaceutical comparability studies. J Pharm Sci 100(6):2071–2086. https://doi.org/10.1002/jps.22432.The
62. Masson GR, Burke JE, Ahn NG et al (2019) Recommendations for performing, interpreting and reporting hydrogen deuterium exchange mass spectrometry (HDX-MS) experiments. Nat Methods 16(7):595–602. https://doi.org/10.1038/s41592-019-0459-y
63. Waterhouse AM, Procter JB, Martin DMA, Clamp M, Barton GJ (2009) Jalview Version 2-A multiple sequence alignment editor and analysis workbench. Bioinformatics 25(9):1189–1191. https://doi.org/10.1093/bioinformatics/btp033
64. Madeira F, Park YM, Lee J et al (2019) The EMBL-EBI search and sequence analysis tools APIs in 2019. Nucleic Acids Res 47(W1):W636–W641. https://doi.org/10.1093/nar/gkz268
65. Robert X, Gouet P (2014) Deciphering key features in protein structures with the new ENDscript server. Nucleic Acids Res 42(W1):320–324. https://doi.org/10.1093/nar/gku316